

Supplementary Figures

Supplementary Figure 1: Sorting strategy, quality control and integration of scRNA-seq datasets of PbTII cells 28 days after infection from two independent experiments.

(A) FACS gating strategy for isolation of PbTII cells from spleen at day 28 post-infection and parasitemia during *PcAS* primary infection in the presence or absence (saline-treated control group) of antimalarial treatment. Data are pooled from 2 independent experiments (n=5/group/experiment).

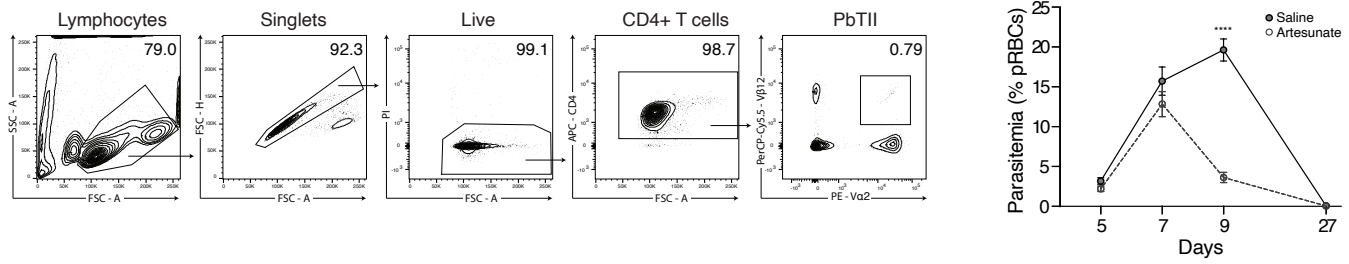
(B) Violin plots showing the distribution of PbTII cells for number of UMIs, proportion of mitochondrial content, and number of genes.

(C) PCA representation of PbTII cells before and after integration using *Seurat*. Cells coloured by experimental origin.

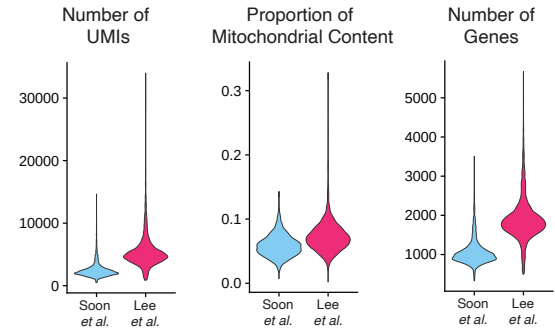
(D) (Left) UMAP representation of PbTII cells after integration using *Seurat* showing the individual clusters from unsupervised clustering (Louvain algorithm). (Right) Bar plot showing frequency of PbTII cells from each experiment in each cluster.

(E) (Left) UMAP representation of PbTII cells after integration using *Harmony*. Cells coloured by experimental origin. (Middle) UMAP representation showing individual clusters from unsupervised clustering (Louvain algorithm). (Right) Bar plot showing the frequency of PbTII cells from each experiment in each cluster.

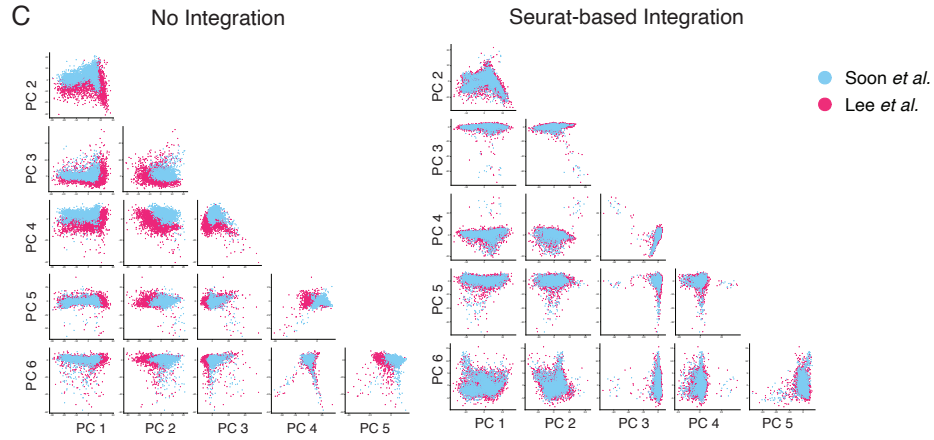
A



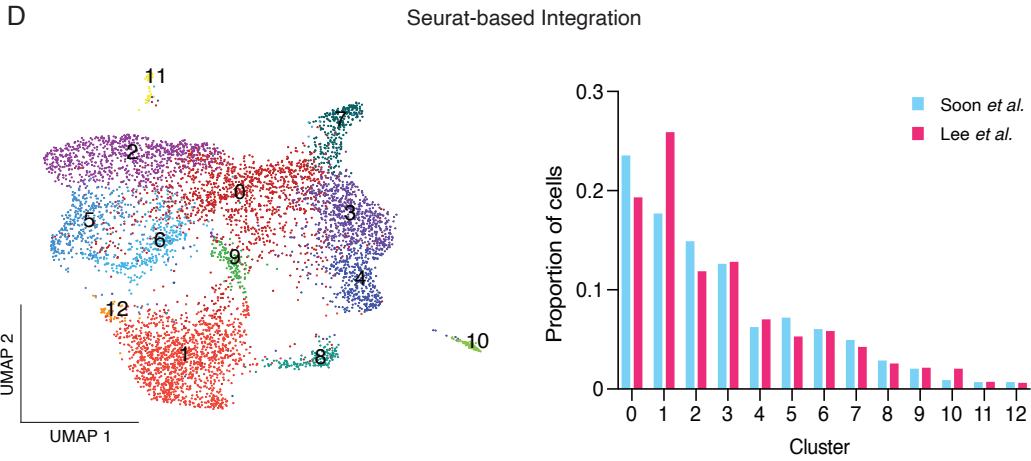
B



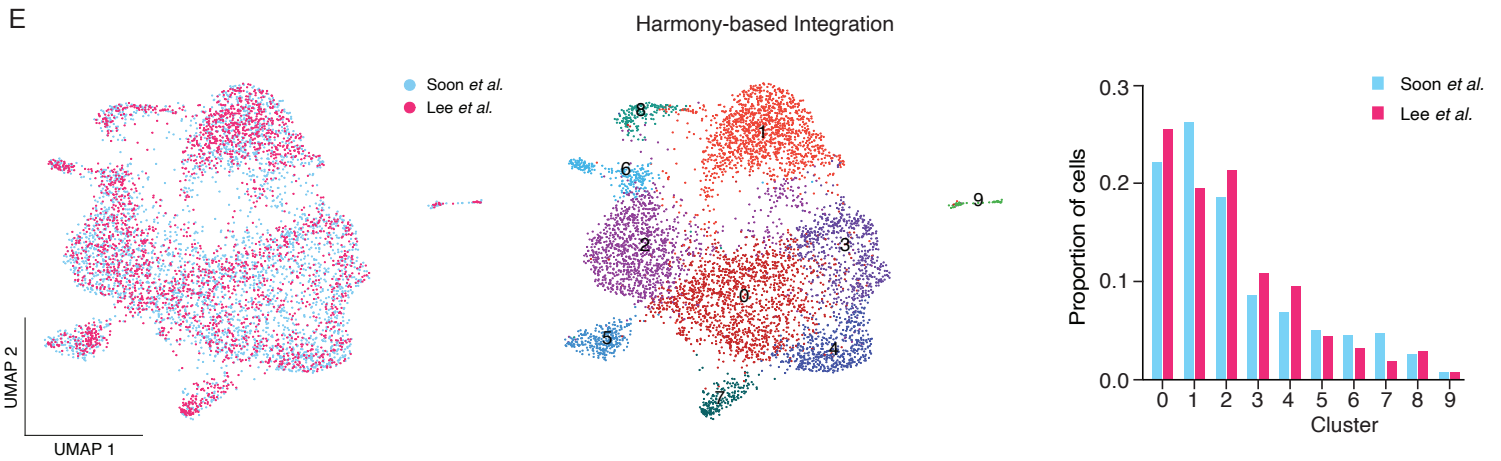
C



D



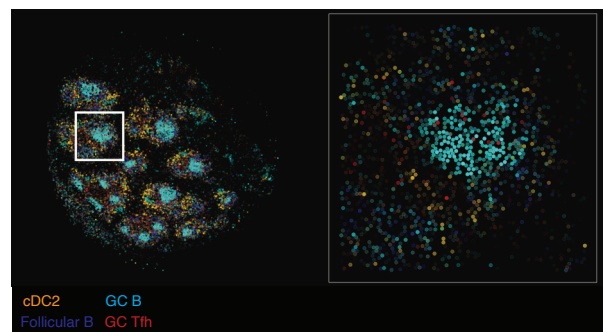
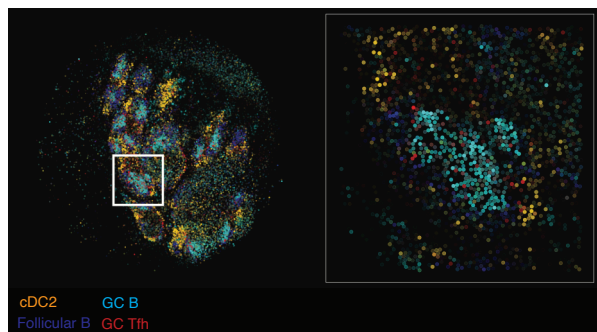
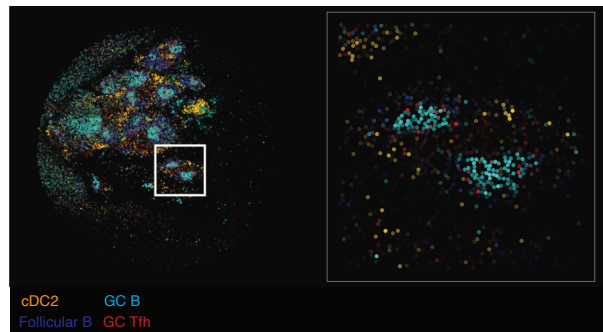
E



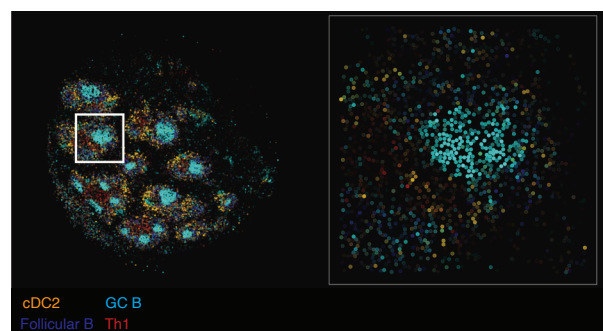
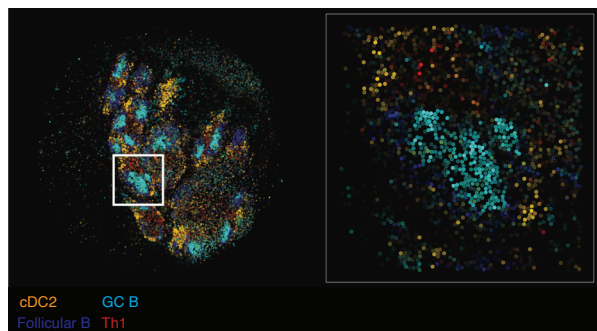
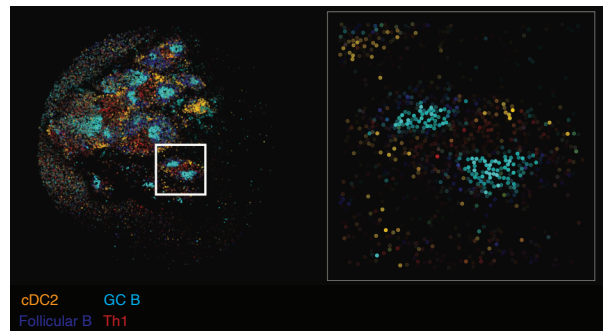
Supplementary Figure 2: Spatial maps of mouse spleen tissue generated using Slide-seqV2 reveal GC Tfh transcriptomes in GC B-cell regions.

Spleens were harvested at day 30 post-infection and processed by *Slide-seqV2* and analysed as in Main Figure 1E. Three independent slides are shown here in three columns, with the same GC B cell, cDC2 and follicular B cell data shown in each panel for a given column, with GC Tfh, Th1 memory or Tcm cells shown in red in each row. These slides are replicates for data shown in Figure 1E.

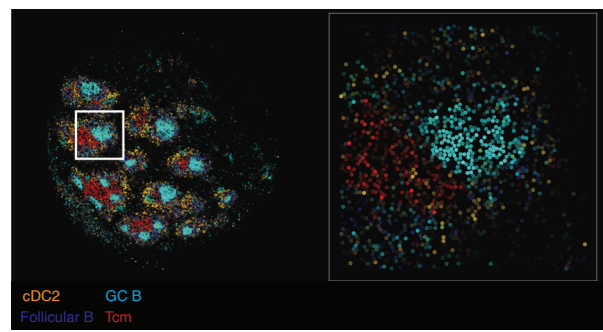
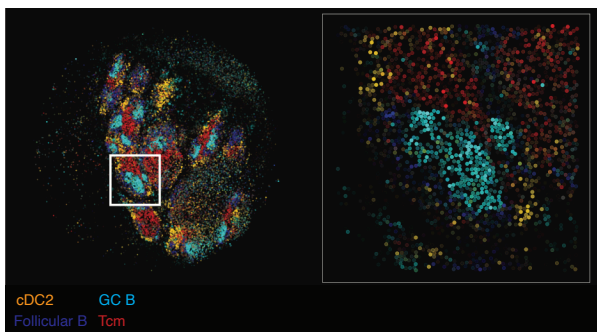
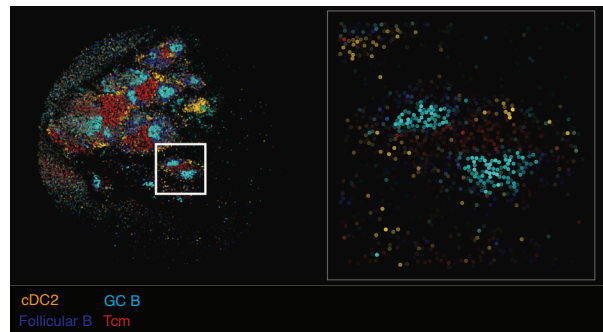
GC Tfh



Th1 memory

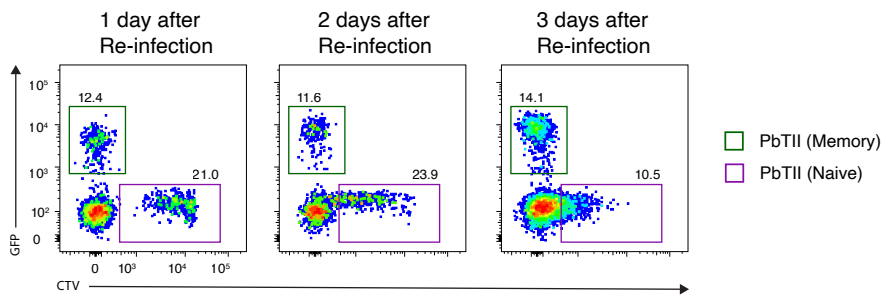
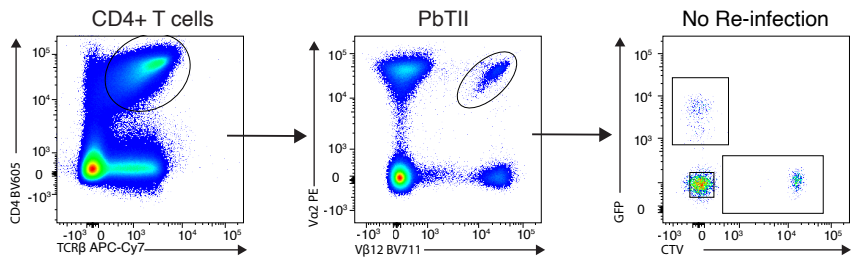
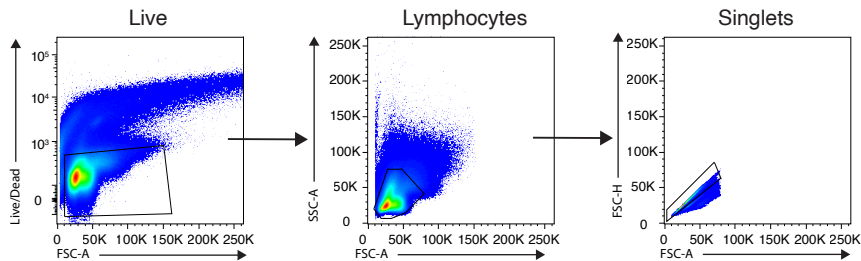


Tcm



Supplementary Figure 3: FACS gating strategy for isolation of antigen-experienced and naïve PbTII cells from spleens at prior to (Top) and 1, 2, and 3 days after re-infection (Bottom).

These data relate to experiments in Main Figures 1 and 2.



Supplementary Figure 4: Co-expression gene network analysis shows transient link of RNA processing with immune effector function and later with proliferation.

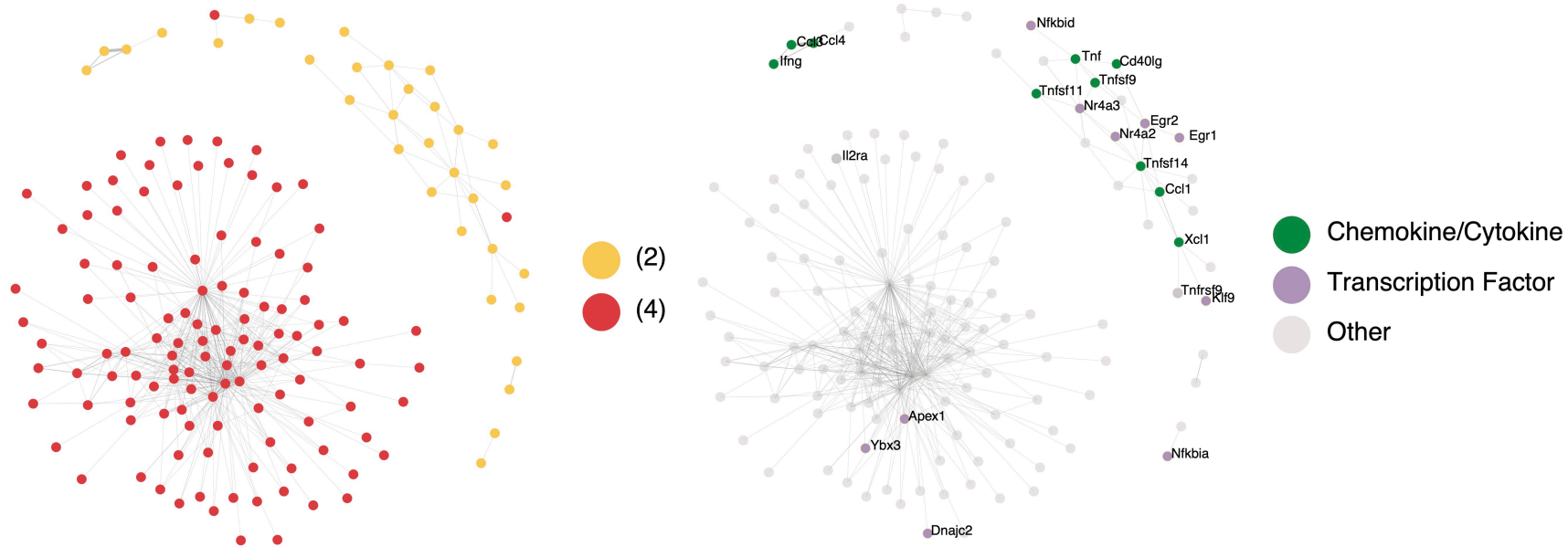
(A) Co-expression network analysis of genes (represented as nodes) in dynamics 2 and 4 using cells from Late pseudotime (in Figure 4A). Nodes are coloured by dynamics of origin (Left) and protein class (Right).

(B) Co-expression network analysis of genes in dynamics 2, 3, 4, and 5 using cells from Mid pseudotime (Left) and Late pseudotime (Right).

Nodes are coloured by dynamics of origin. Edge weight corresponds to Spearman's rho values (only showing $\rho > 0.2$).

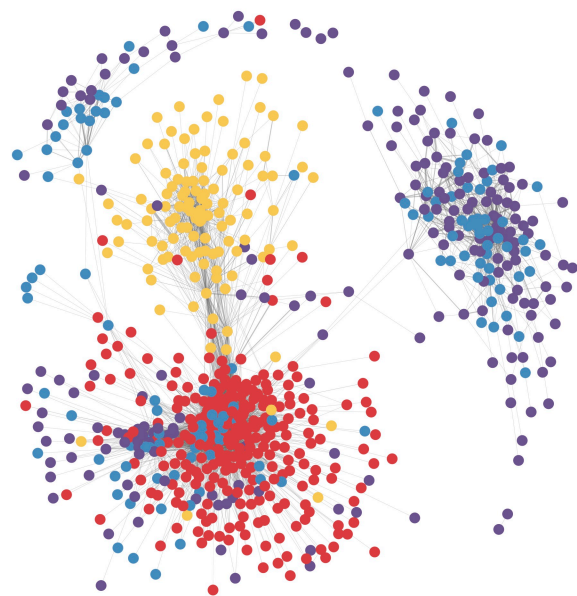
A

Late pseudotime

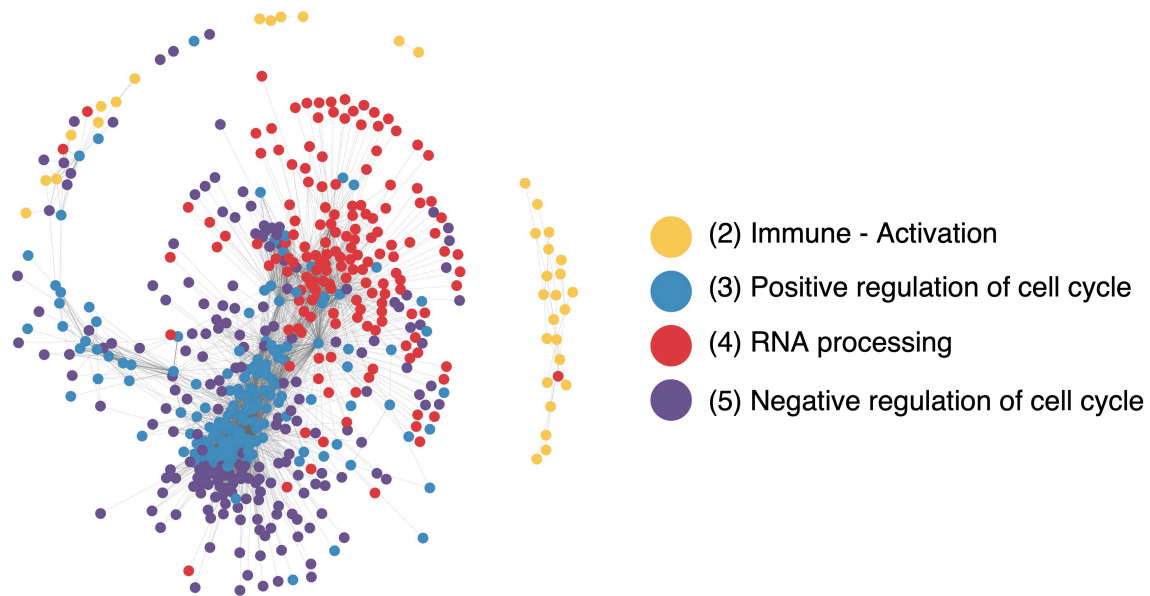


B

Mid pseudotime



Late pseudotime



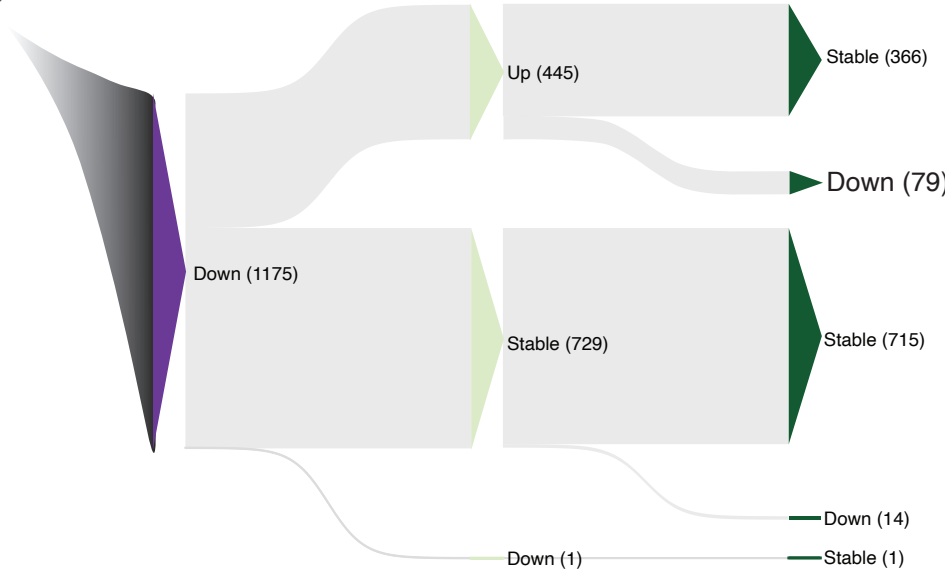
Supplementary Figure 5: Expression dynamics during memory transition and recall for 1175 genes initially downregulated during primary Th1 differentiation.

Sankey plot schematic showing expression dynamics for the 1175 genes initially downregulated in primary Th1 cells relative to naïve PbT1s (Up: upregulated, Down: downregulated, Stable: no significant change) at each stage in reference to the preceding stage. Full list of genes downregulated from Th1-memory to recall are shown on the right.



Down-regulated in Primary Day 7 -Th1

Naive Primary Memory Recall



Zbtb20	2510002D24Rik	Bzw2	Rabac1
Cirbp	Gm11808	Tra2a	Lpar6
Rps21	Bcl2	Fam189b	Zfp950
Ccm2	Hvcn1	Mfng	Mfap1a
Bcl11b	Rps27	Clk1	Cd40lg
Rps27rt	Pcmtd1	Zcchc11	Slc38a2
Tcf7	Apbb1ip	Clec2i	Lamp1
Znr1	Jun	Zfp398	Prkacb
Zfp36l2	Ii7r	Uvr3g	Mbp
Pdcd4	Skap1	Zfp68	lfnar2
Chd3	4930523C07Rik	Rasgrp1	Nisch
Rassf2	Ankrd10	Crtc3	Mbnl1
Izumo4	Srsf5	Clip1	Sesn3
Uba52	St8sia4	Sit1	Rasal3
Zfp644	Ltb	Rcbtb2	Ggnbp2
Taf7	Cd96	Fbxl12	Tmem191c
Eif4a2	Zfp652	Csnk1g2	Dpm1
lkbkb	Rbm4b	Inpp4b	Asap1
Rab11fip2	Rab37	Nr3c1	Adgre5
Hmha1	Avl9	Nufip2	

Sell

Supplementary Figure 6: Quality control for scRNA-seq/TCR-seq dataset of CD11a^{hi}/CXCR3⁺ polyclonal CD4⁺ T cells prior to and 3 days after re-infection.

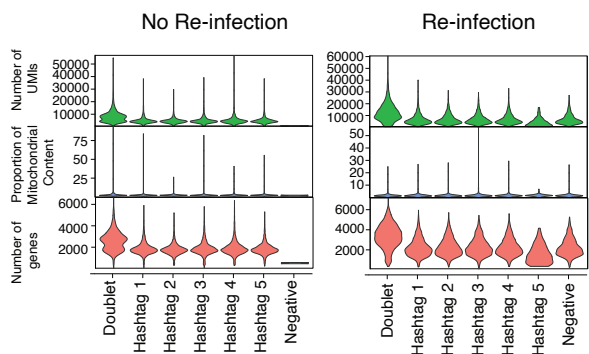
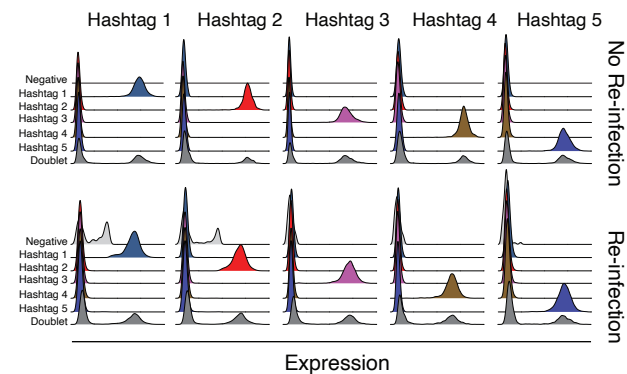
(A) (Top) Ridge plots showing enrichment of hashtag oligos (columns) for negative, singlet (Hashtags 1-5), and doublet groups (rows). Each hashtag represents data from one mouse. (Bottom) Violin plots showing distribution of polyclonal CD4⁺ T cells for number of UMIs, proportion of mitochondrial content, and number of genes detected.

(B) (Top) UMAP of polyclonal CD4⁺ T cells prior to and after re-infection before removal of TCR genes. Cells are coloured by clusters from unsupervised clustering (Louvain algorithm). (Bottom) Dot plots showing expression of TCR genes from top 5 marker genes of each cluster. Colour represents mean normalised expression and size of dots represents percentage of cells expressing these genes.

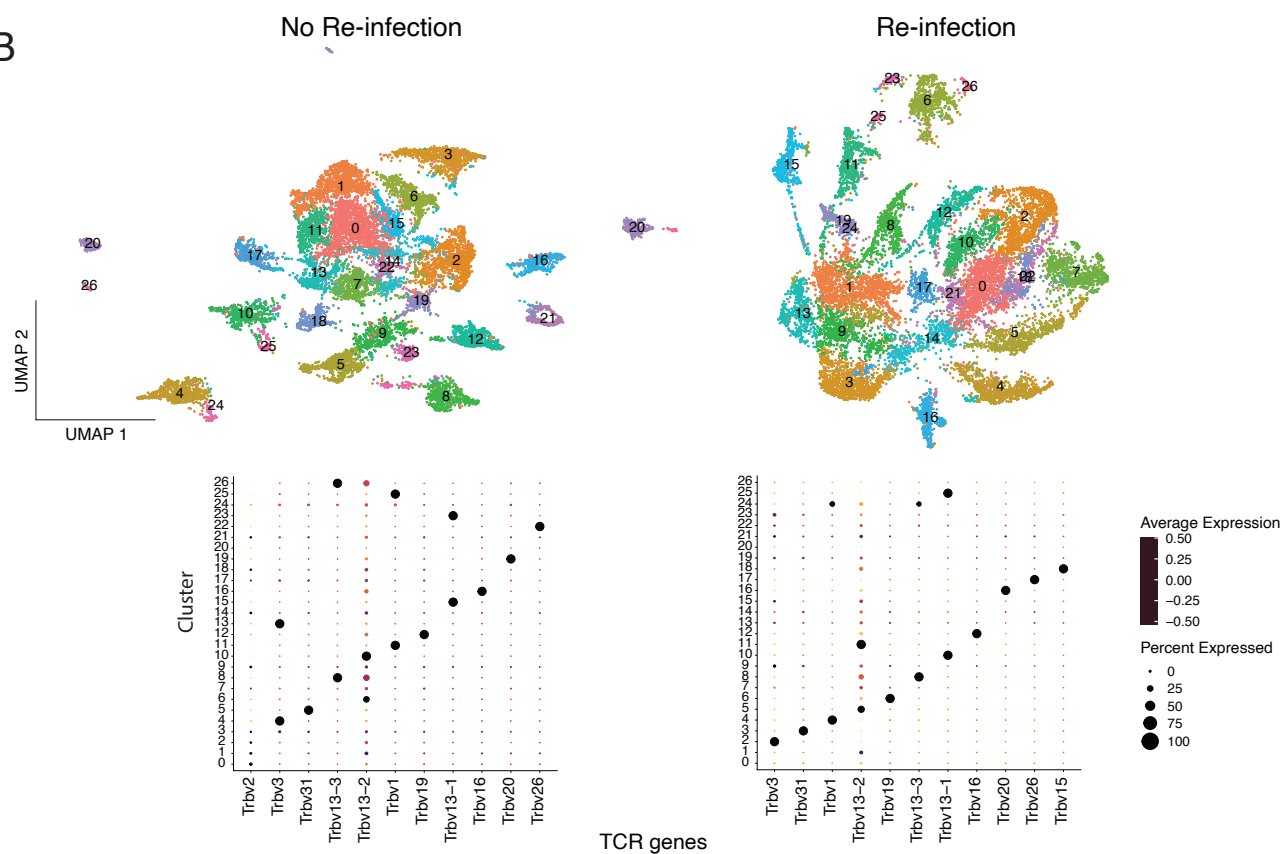
(C) (Top) UMAP of polyclonal CD4⁺ T cells after removal of TCR genes. Cells coloured by clusters from unsupervised clustering (Louvain algorithm). (Bottom) Violin plots showing distribution of polyclonal CD4⁺ T cells for number of UMIs, proportion of mitochondrial content, *Cd74* expression, and *Cd8a* expression.

(D) UMAP of polyclonal CD4⁺ T cells expressing *Cxcr3* and *Zbtb16* after removal of clusters with high *Cd74* and *Cd8a* expression (shown in **(C)**).

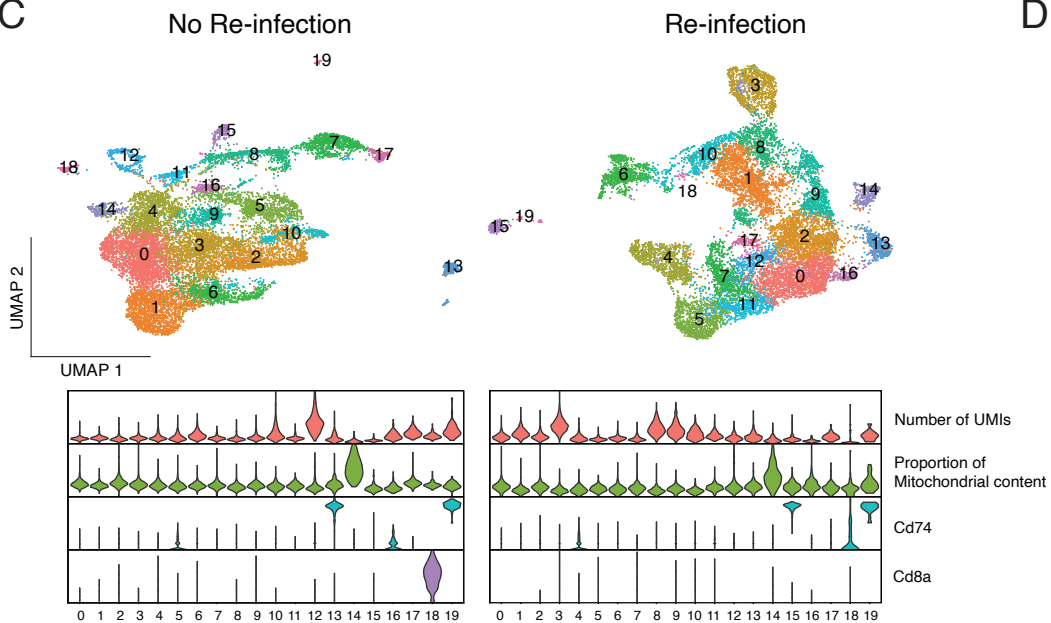
A



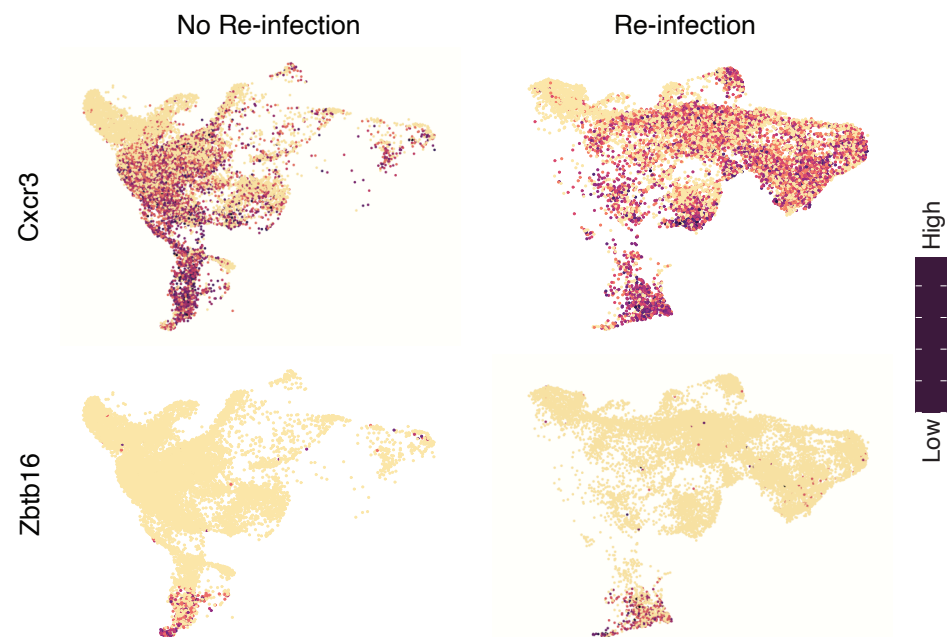
B



C



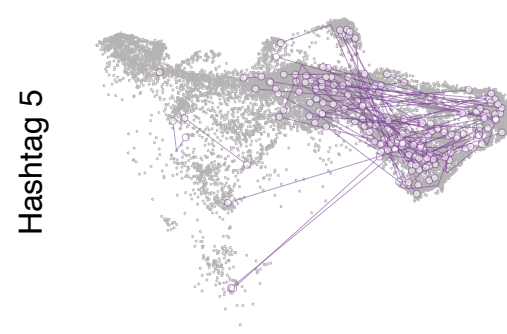
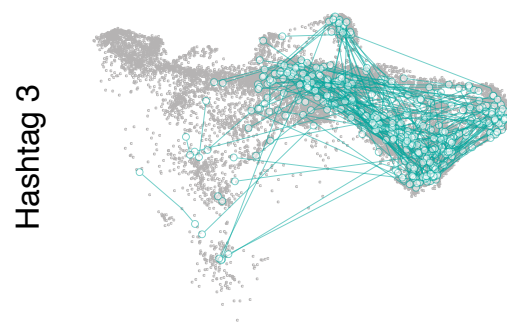
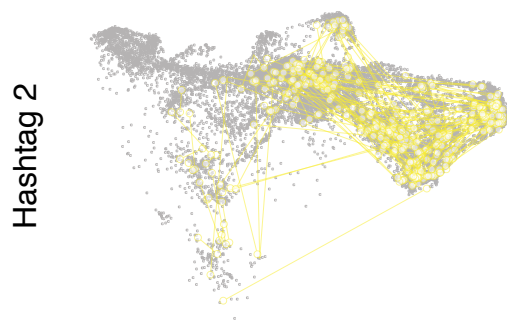
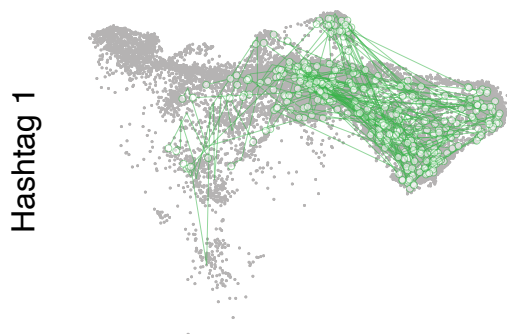
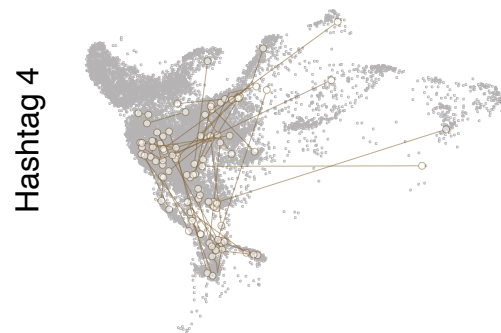
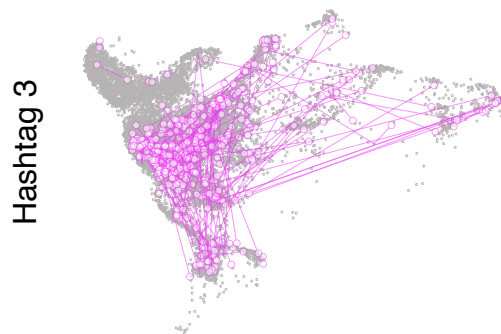
D



Supplementary Figure 7: Clonal relationships of polyclonal CD4⁺ T cells prior to and after re-infection
UMAP representation of CD11a^{hi}/CXCR3⁺ polyclonal CD4⁺ T cells (with 5% spike in of CD11a^{lo}/CXCR3⁻ naïve cells) for 5 mice prior to re-infection, and 5 mice after re-infection. Cells sharing the same TCR chains are connected by edges and only families with four or more cells sharing the same TCR chains are shown on the plot. Each hashtag represents data from one mouse.

No Re-infection

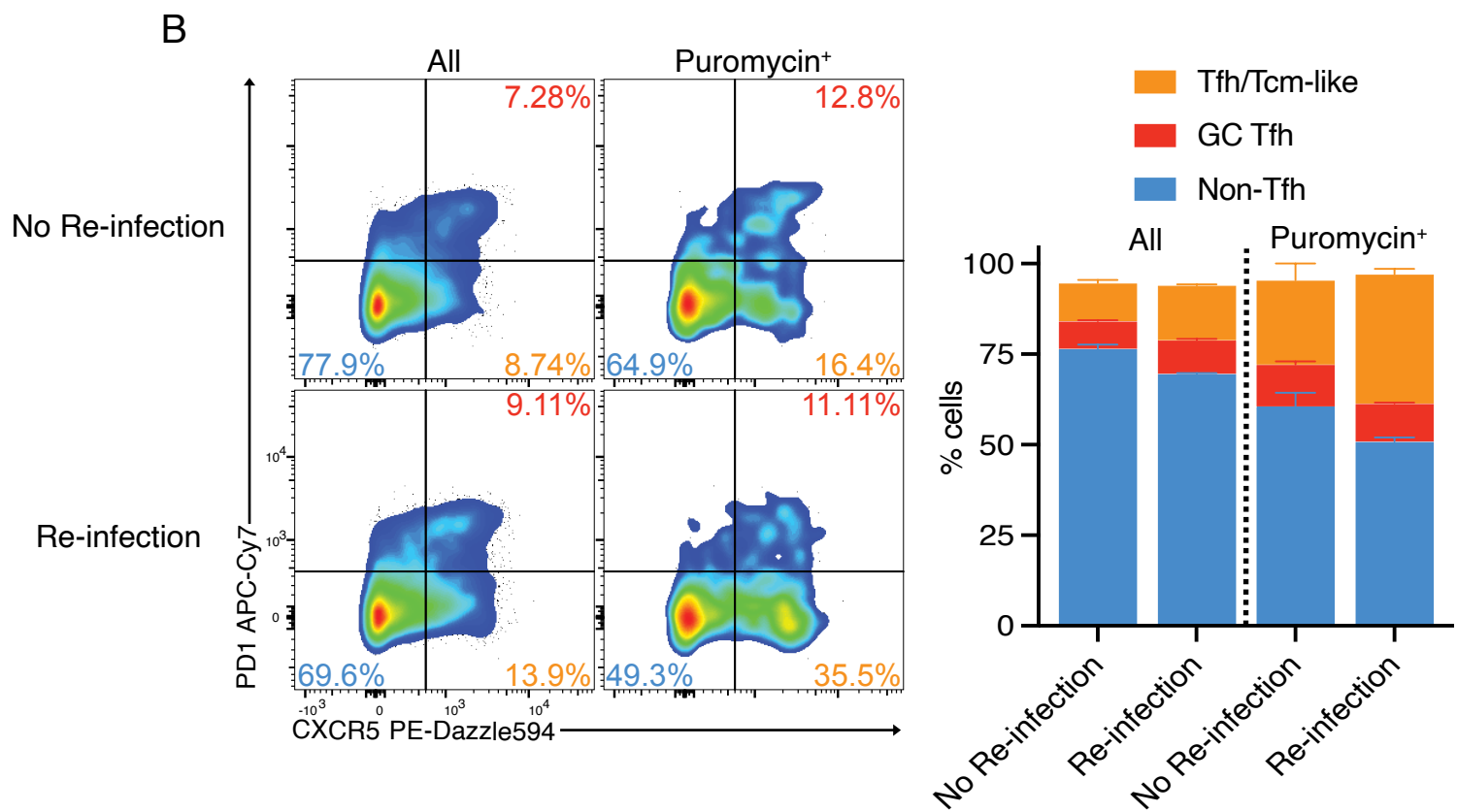
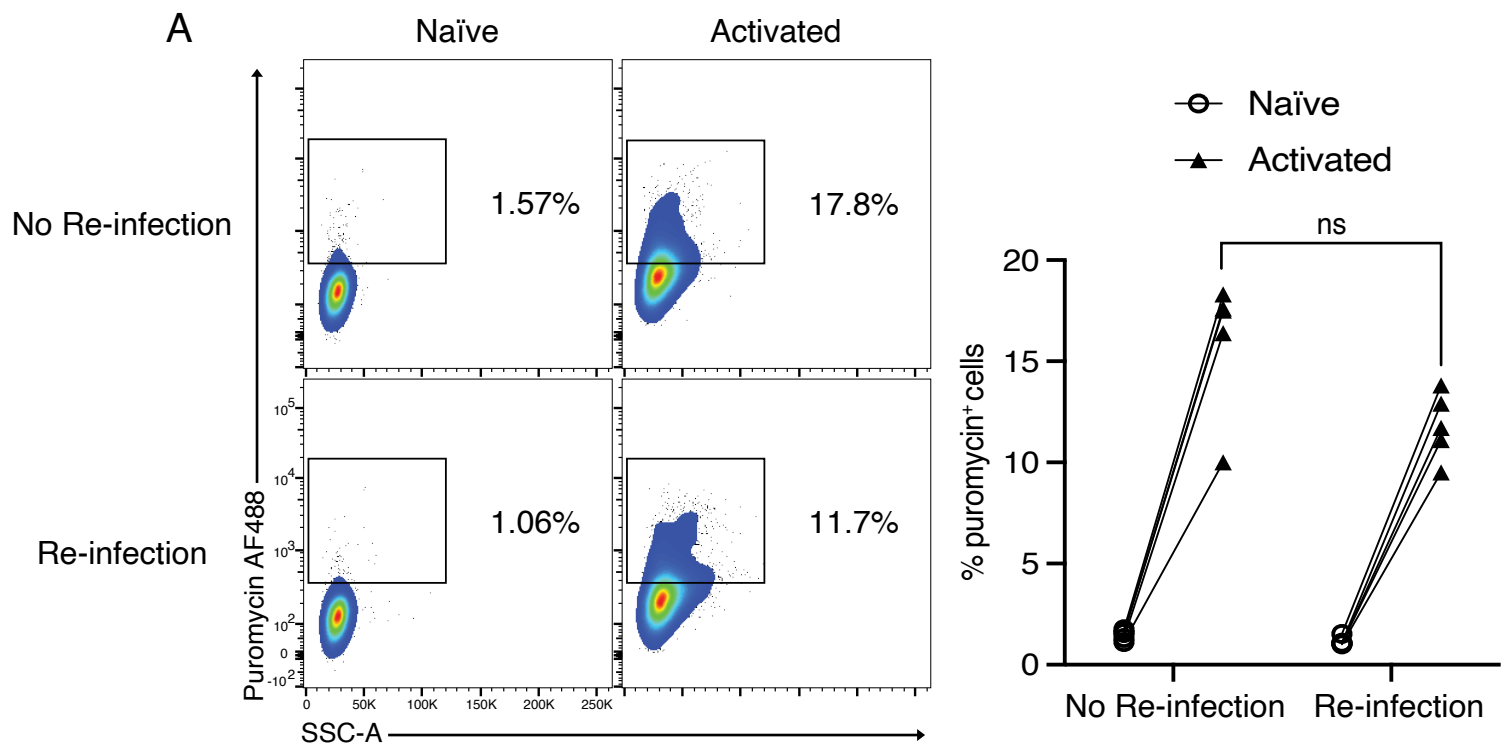
Re-infection



UMAP 2

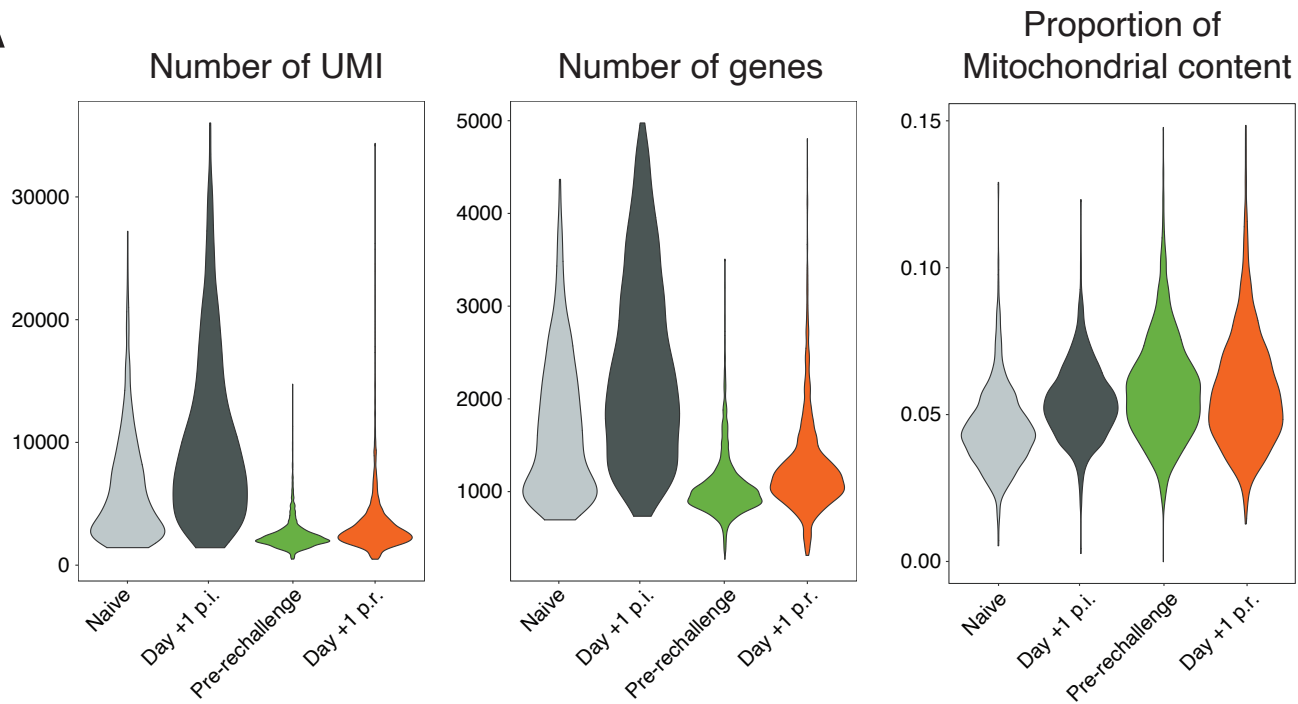
UMAP 1

Supplementary Figure 8: Antigen-experienced polyclonal CD4⁺ T cells do not increase protein translation 24 hours after re-infection. (A) Representative FACS plots showing puromycin binding for paired naïve (CD11a^{lo} CXCR3^{lo}) naïve versus and activated polyclonal splenic CD4⁺ T cells prior to and 24 hours after re-infection. Graph shows % puromycin⁺ cells for individual mice (n=5 mice/group). Statistical analysis was performed using a non-parametric Mann-Whitney test (ns= not significant). Data representative of two independent experiments showing similar results. **(B)** Representative FACS plots of PD1 & CXCR5 expression in total (left panels) and puromycin⁺ (right panels) activated, polyclonal CD4⁺ T cells prior to and 24 hours after re-infection. Stacked bar graph showing the percentages of Tfh/Tcm-like, GC Tfh, and non-Tfh subsets. Data representative of two independent experiments showing similar results.

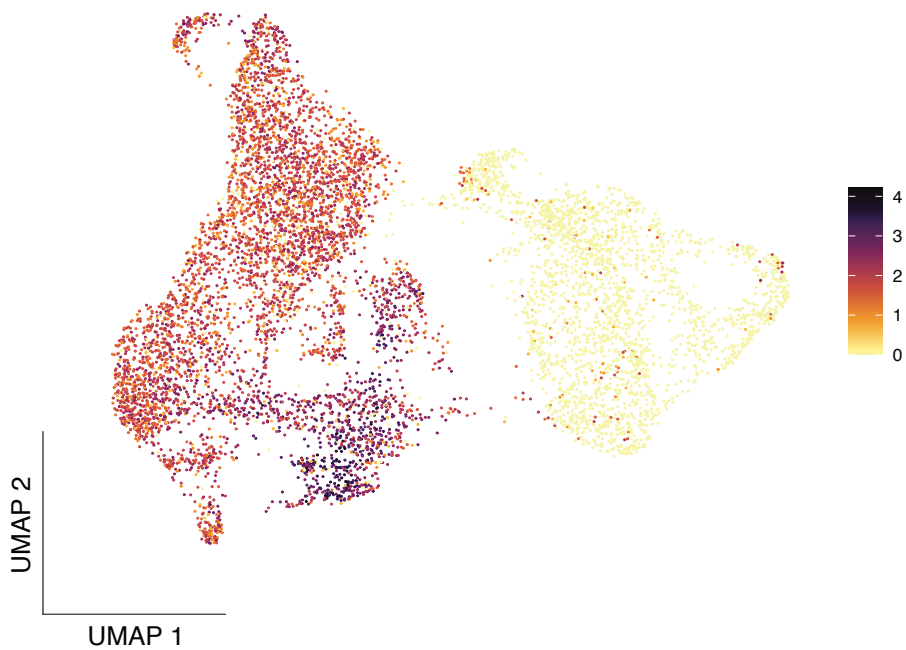


Supplementary Figure 9: Quality control of scRNA-seq data for antigen- experienced and naïve PbTII cells prior to and 1 day after re-infection (A) Violin plots showing the distribution of PbTII cells for number of UMIs, proportion of mitochondrial content, and number of genes. **(B)** UMAP visualisation of *egfp* expression, denoting antigen- experienced PbTIIs.

A

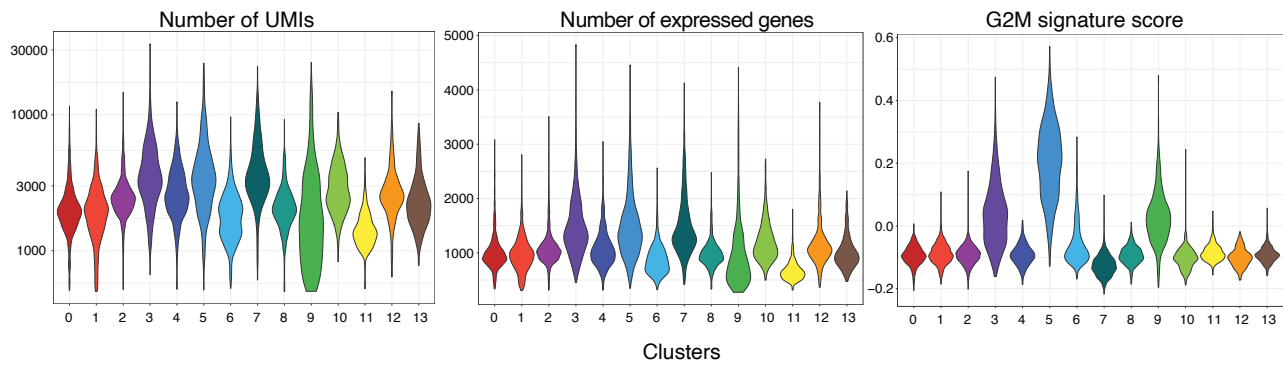


B

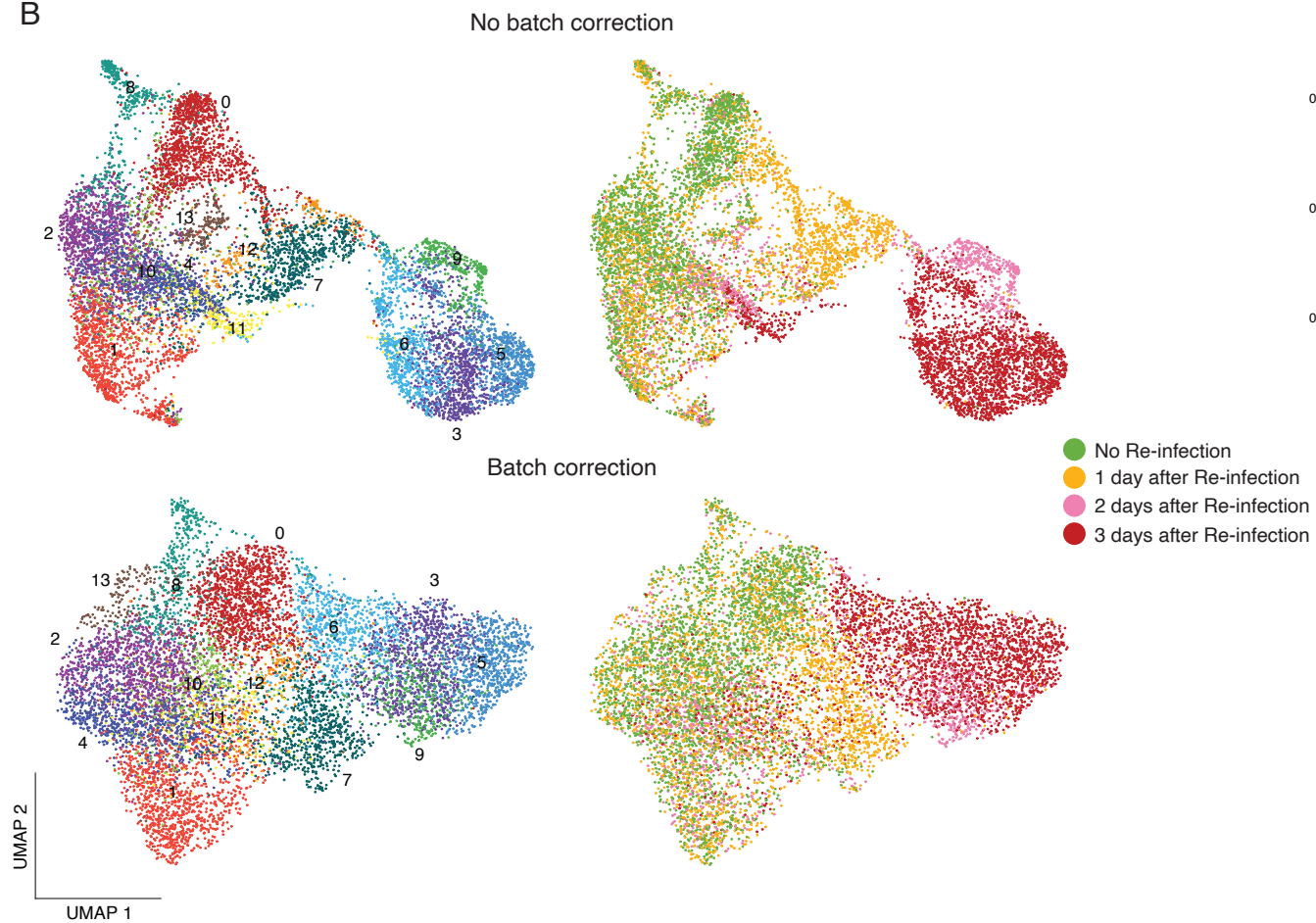
egfp

Supplementary Figure 10: Quality control of scRNA-seq data for PbTII cells prior to and 1, 2, and 3 days after re-infection. (A) Violin plots showing the distribution of PbTII cells for number of UMIs, number of genes, and G2M phase signature score for each cluster. **(B)** UMAP representation of PbTII cells before (Top) and after (Bottom) integration using scVI. Cells are coloured by clusters from unsupervised clustering (Leiden algorithm) (Left) and timepoint (Right). **(C)** Violin plots showing the distribution of PbTII cells for number of UMIs, proportion of mitochondrial content, number of genes, and *egfp* expression for each sample after removal of cluster 9 in **(A/B)**.

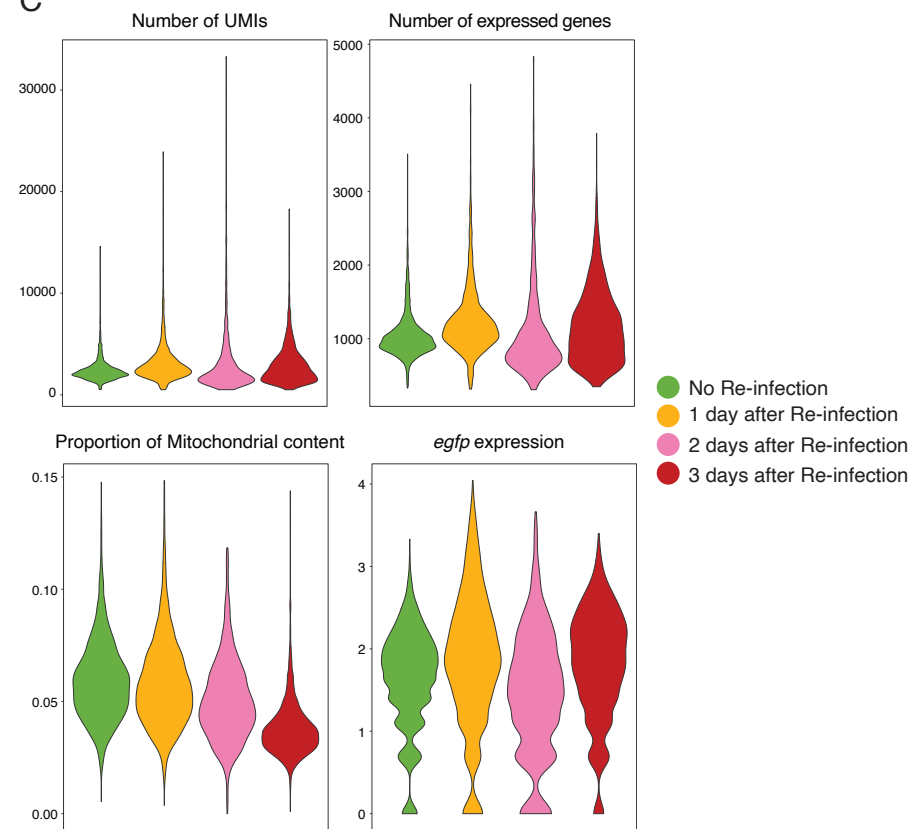
A



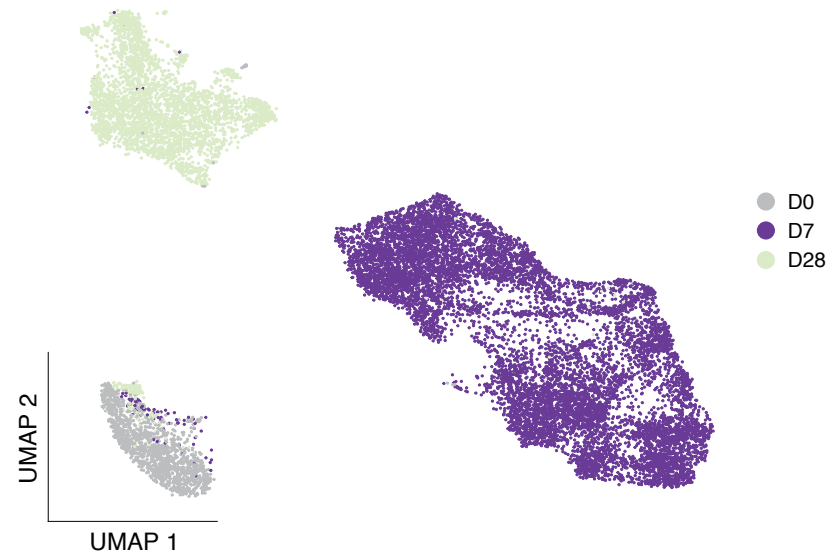
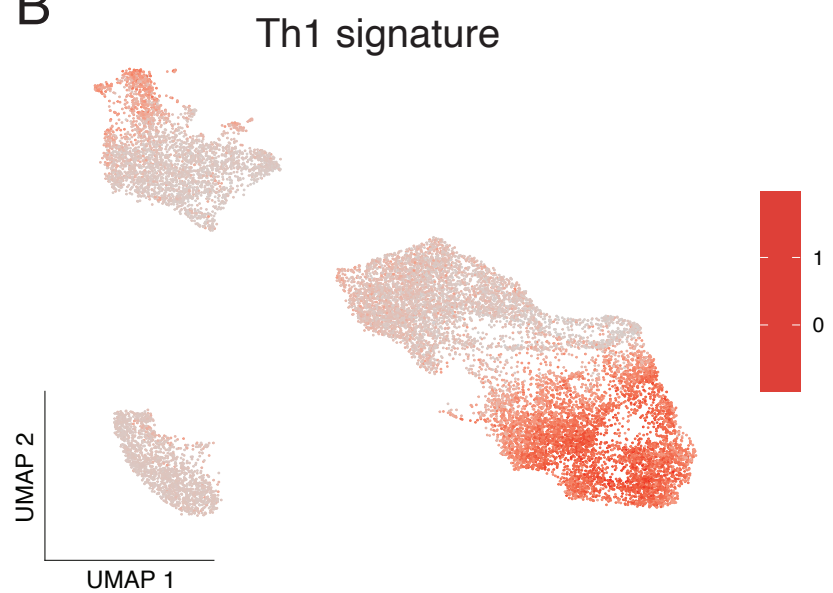
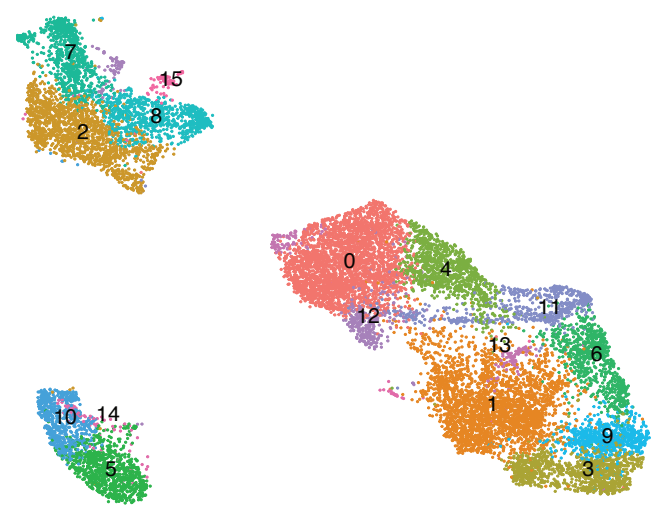
B



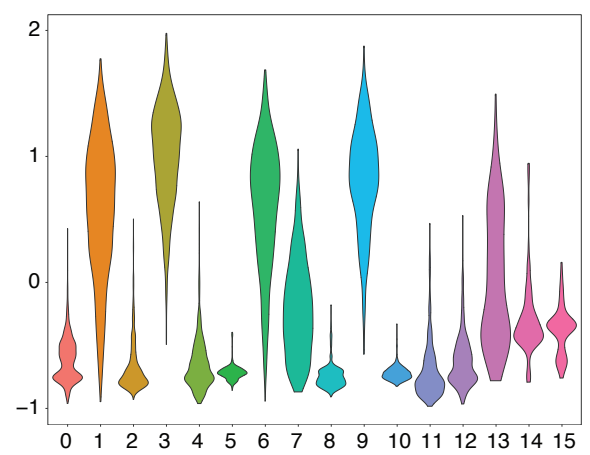
C



Supplementary Figure 11: Analysis of scRNA-seq data of naïve and effector PbTII cells at day 7 post-infection, compared with day 28 post-infection (Soon *et al.* 2020). (A) UMAP representation of PbTII cells. Cells are coloured by sample of origin. **(B)** UMAP visualisation of PbTII cells expressing Th1 signature score. **(C)** (Left) UMAP representation of PbTII cells. Cells are coloured by clusters from unsupervised clustering (Louvain algorithm) and (Right) violin plot showing the distribution of PbTII cells for Th1 signature score for each cluster in **(B)**.

A**B****C**

Th1 signature



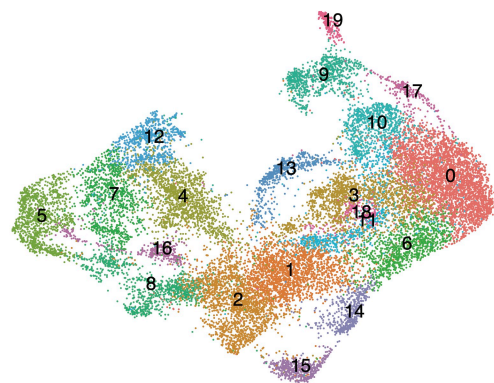
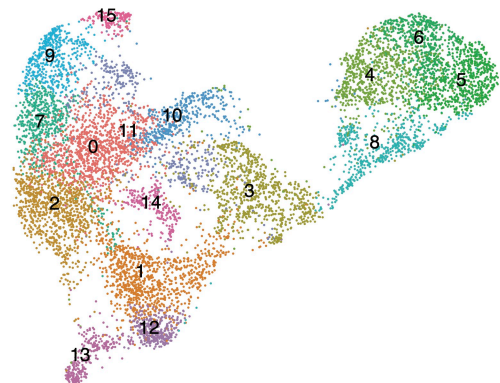
Supplementary Figure 12: Integration of scRNA-seq datasets of PbTII cells and polyclonal CD4⁺ T cells prior to and 3 days after re-infection to identify cell clusters of similar phenotypes. (A) (Top) UMAP representation of PbTII cells and polyclonal CD4⁺ T cells prior to data integration. Cells are coloured by clusters from unsupervised clustering. (Bottom) Combined and integrated UMAP representation generated using scVI. Cells are coloured by clusters from unsupervised clustering (Louvain algorithm) of PbTII cells (Left) and polyclonal CD4⁺ T cells (Right). **(B)** Visualisation of Th1, Tcm, and Tfh signature scores on the integrated UMAP shown in **(A – Bottom)**.

A

No batch correction

PbTII

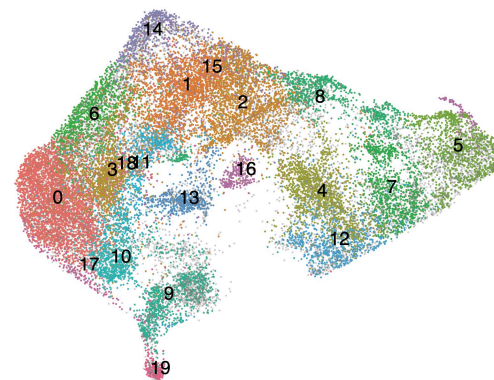
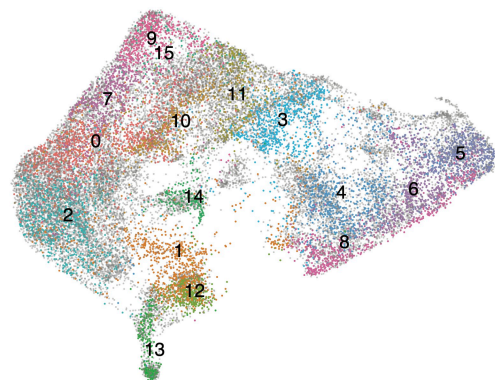
Polyclonal



Batch correction

PbTII

Polyclonal



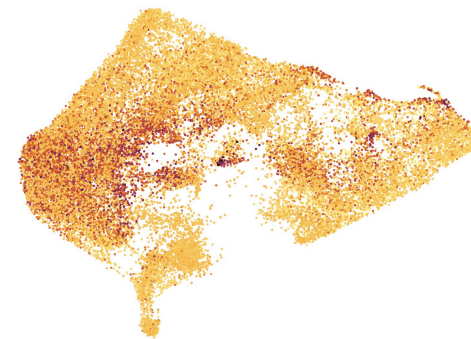
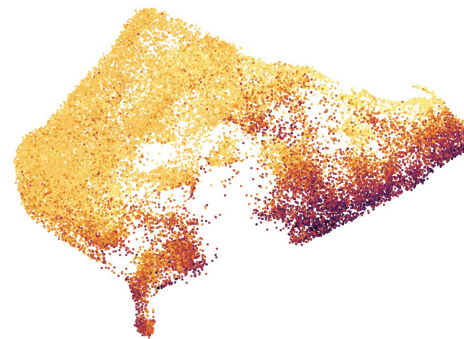
UMAP 2

UMAP 1

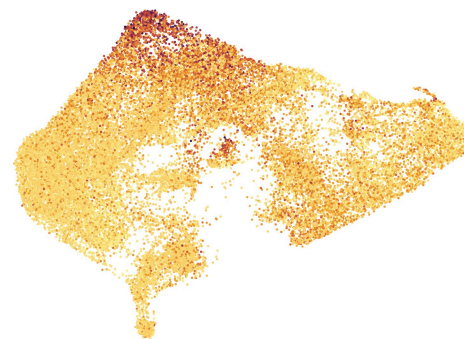
B

Th1 signature

Tcm signature



Tfh signature



UMAP 2

UMAP 1